

Hole doping in high temperature superconductors using the XANES technique

N M Hamdan¹ and Z Hussain²

¹ Physics Department, American University of Sharjah, Sharjah 26666, United Arab Emirates

² Advanced Light Source, LBNL, Berkeley, CA 94720, USA

E-mail: nhamdan@aus.edu

Received 1 September 2008, in final form 24 November 2008

Published 28 January 2009

Online at stacks.iop.org/SUST/22/034007

Abstract

Superconducting and physical properties of F-doped HgPb-1223 and Ce-doped Tl-1223 systems were considerably improved through adjusting the hole content of the two systems. In this study, we have used the x-ray absorption near-edge structure (XANES) technique to investigate the electronic structure of the two systems by probing the unoccupied electronic states. For the F-doped Hg-1223 system, the O K-edge, Ca L_{2,3} and Cu L_{2,3}-edge structures were thoroughly investigated. The pre-edge features of O K-edge spectra, as a function of doping, reveal important information about the projected local density of unoccupied states on the O sites in the region close to the absorption edge, which is a measure of O 2p hole concentration in the valence band. In the originally under-doped Hg-1223, the results indicate that the number of O 2p holes in the CuO₂ planes increases as fluorine was introduced up to an optimal value, after which it decreases. Furthermore, the Cu L_{2,3} absorption edge provides useful information about the valence state of Cu which is also related to the hole density in the CuO₂ planes and confirms the same previous conclusion. The Ca L_{2,3}-edge shows the presence crystal field splitting in HgPb1223/F_x which is similar to CaF₂ and CaO in addition to the spin-orbit splitting of the Ca 2p core level electrons. These results ensure that fluorine goes into the structure of HgPb-1223/F_x and it occupies the vacant interstitial oxygen site in the Hg-O plane, as was expected. In Ce-substituted Tl-1223, similar measurements were performed for samples with different Ce content. The pre-edge feature of the O K-edge spectra shows clearly the drastic decrease of the hole content in CuO₂ planes of this originally over-doped system with increasing Ce content. This result is also confirmed from the chemical state of Ce in the structure as obtained from the Ce M_{4,5}-edge spectra.

(Some figures in this article are in colour only in the electronic version)

1. Introduction

Hole concentration in CuO₂ planes of high temperature superconductors plays an important role in determining their superconducting and normal state properties [1, 2]. The transition temperature (T_c) of most high temperature superconductors and the critical current densities are sensitive to the number of holes in the CuO₂ planes. Controlling the hole content in the CuO₂ planes can be achieved by different methods: anion substitution (fluorine for oxygen, for example), cation substitution and oxygen non-stoichiometry that can be

achieved either by varying the annealing conditions or by irradiation effects. In this work, we will consider anion and cation substitution in Hg-based and Tl-based compounds, respectively. Tl-based and Hg-based superconductors are particularly sensitive to the number of holes in the CuO₂ planes, especially for the technologically important Tl-1223 and HgPb-1223 phases. Usually, as-prepared samples of Tl-1223 are over-doped, while samples of HgPb-1223 are under-doped. Optimizing the hole concentration in these systems had been the concern of several groups [3–6]. Cation substitutions for various elements in these compounds were

performed in attempts to control the hole concentration in the CuO_2 planes and to increase T_c . Although this method has been extensively used by many groups for all known high temperature superconducting systems, it sometime poses serious problems. These problems are related to the fact that the substituted cation can enter the structure at various and multiple atomic sites and therefore can affect the stoichiometry and cause the formation of unwanted impurity phases. We have performed anion substitution for both the over-doped Tl-1223 and the under-doped Hg-1223 systems. Oxygen was partially replaced with the more electronegative fluorine in the Tl-1223 system. We have achieved significant enhancements of both the transition temperature and the critical current density in this system [1, 7, 8]. Furthermore, considerable improvements of the phase formation and normal state properties have been achieved. These enhancements were attributed to optimizing the hole concentration in the CuO_2 planes. We have also studied the effect of Ce substitution for Sr in samples that consist of the two phases Tl-1223 and Tl-1212 [9, 10]. We have also observed an enhancement of the superconducting properties for small values of Ce concentration x , followed by a deterioration in the superconducting properties for higher values of x .

Mercury-based high temperature superconductors are unique among other cuprate superconductors, because they have the highest T_c so far, and T_c strongly depends on the applied hydrostatic pressure. $\text{HgBa}_2\text{Ca}_2\text{Cu}_3\text{O}_{8+\delta}$ (Hg-1223) have T_c above 130 K under ambient atmosphere and it increases to above 160 K under high pressure [11]. This property has led to considerable research activities on this system. Structural investigations under high pressure have revealed a drastic shortening of the apical Cu-O distance, which is possibly linked to the increase in T_c [12]. Neutron diffraction results have also shown that excess oxygen has the same effect on the crystal structure of this compound as that when subjected to high pressure [13]. On the other hand, band structure calculations using the local density approximation (LDA) have predicted an increase in T_c with the increase in the density of holes in the Cu-O planes [14]. This is equivalent to insertion of excess oxygen into the HgO_δ planes [15, 16]. Novikov and Freeman have also observed similar effects on the position of the Hg $6p_z$ and the O $2p_z$ state near the Fermi level [16]. The variation of the excess oxygen δ modifies the charge carrier concentration in the CuO_2 planes and hence changes T_c [17].

It is well established that the substitution of transition elements such as Pb, Re and Bi for Hg simplifies the synthesis, and improves and stabilizes the phase formation of Hg-based superconductors [18–20]. Furthermore, partial substitution of mercury by a high valence transition metal introduces extra oxygen atoms in the HgO_δ plane [17], and hence improves its superconducting properties. It was also established that partial substitution of Pb, Re or Bi for Hg does not drastically increase the transition temperature T_c as expected from high-pressure measurements. This made us believe that there is still a possibility of further improving the superconducting properties, which could be attempted by anion substitution. Therefore, and because we have

achieved considerable improvements in the superconducting properties and phase formation of Tl-1223 through fluorine substitution [1, 21–24], we have attempted to optimize the properties of Hg-1223 by introducing fluorine into the structure for both the Pb-doped (HgPb-1223 and the Re-doped HgRe-1223). In this work we will restrict our discussions to the HgPb-1223 system. Although Tl-1223 and HgPb-1223 phases have similar structures, there is a major difference that affects the hole distribution in the CuO_2 planes and hence the electronic structure of both compounds [21–25]. This difference is in the O site of Tl-O and the corresponding Hg-O planes where it is fully occupied and partially filled in Tl-1223 and Hg-1223, respectively. Therefore, fluorine was introduced in the Cu-O planes in the case of Tl-1223 but it was expected to fill the partially filled site in the Hg-O planes in Hg-1223. This led to increasing the hole concentration of the originally under-doped Hg-1223, and to decreasing it in the over-doped Tl-1223 [21–26].

We have also achieved considerable improvements in the critical current density of both Re- and Pb-doped Hg-1223, and a 2 K increase in T_c , by incorporating fluorine into the structure in the case of fluorinated Pd-doped Hg-1223 [26, 28]. Putilin *et al* and Lockshin *et al* [28, 29] have observed a 4 K enhancement in the transition temperature of fluorinated Hg-1223. Wang and Hermann have also observed a considerable increase in the hysteresis magnetization of fluorinated Hg-1223 [30]. Our structural, electrical and magnetic measurements in both fluorinated Tl-based and Hg-based systems have demonstrated that the observed improvement in the properties of these two systems with fluorine addition are due to changes of the number of charge carriers in the CuO_2 planes [21–24, 26, 27].

Because of the importance of understanding the role of the density of holes in CuO_2 planes, and its relation to filling the partially vacant oxygen site in the Hg-O_δ plane, and the dependence of T_c on the value of δ [32], detailed measurements of electronic structural features in the Hg-1223 system are necessary. The hole state that is directly related to the Hg $6p_z$ hybridization with O(2) $2p_z$ states [32], and the valence state of Cu, are among the electronic properties that could be investigated by near-edge x-ray absorption fine structure measurements. Therefore, we have investigated the effect of fluorine addition on Pb-doped Hg-1223 (HgPb-1223/ F_x) on the XANES spectra (O K-edge, Cu $L_{2,3}$ -edges, Ca $L_{2,3}$) for samples with different fluorine content x . We will also present in this work XANES spectra at the O K-edge, Cu $L_{2,3}$ -edges and Ce $M_{4,5}$ -edges for $(\text{Tl}_{0.5}\text{Pb}_{0.5})\text{Sr}_{2-x}\text{Ce}_x\text{Ca}_2\text{Cu}_3\text{O}_{10}$ samples. The purpose of this part of the work is to demonstrate that the Ce substitution in Tl-1223 reduces the hole concentration in the CuO_2 planes and hence affects the superconducting properties of Tl-1223. This is done by measuring the valence state of Ce in the structure and the projected local density of unoccupied states on the O sites in the region very close to the absorption edge which is a measure of O $2p$ hole concentration in the valence band.

2. Experimental details

The solid state reaction technique in sealed quartz tubes was used to prepare the single-phase Hg-1223 samples with different fluorine contents used in this study. Samples with composition $\text{Hg}_{0.8}\text{Pb}_{0.2}\text{Ba}_2\text{Ca}_2\text{Cu}_3\text{O}_{8+\delta}/\text{F}_x$ (HgPb-1223/ F_x) were prepared with nominal fluorine content ($x = 0.000, 0.050, 0.120, 0.185, 0.285$ and 0.500). The transition temperatures (T_c) for samples with different fluorine content were determined from magnetization versus temperature measurements using a SQUID magnetometer. T_c for some of the samples was double-checked by measuring the resistivity versus temperature utilizing the four-point probe technique. The critical current density determined from magnetic hysteresis and Bean's critical state model has also been determined from hysteresis loops measured also by SQUID in magnetic fields up to 5.5 T. The phase formation and the microstructure of the samples have also been modified through fluorine inclusion that was evident from large size, platelet-like grains. Details of the preparation and characterization of the samples were published elsewhere [26, 27].

Six samples with nominal composition of $(\text{Tl}_{0.5}\text{Pb}_{0.5})\text{Sr}_{2-x}\text{Ce}_x\text{Ca}_2\text{Cu}_3\text{O}_{10}$ were prepared by the solid state reaction technique with $x = 0.0, 0.1, 0.2, 0.3, 0.4$ and 0.5 . Details of the preparation were published elsewhere [8, 9]. The samples were characterized using resistivity, magnetization, scanning electron microscopy, EDS and x-ray diffraction measurements.

The x-ray absorption measurements at the O K-edge, Ca $L_{2,3}$ -edge, Ce $M_{4,5}$ -edges and Cu $L_{2,3}$ -edges were carried out at beamline 9.3.2 at the Advanced Light Source, Lawrence Berkeley National Laboratory. The beamline is equipped with a spherical grating monochromator (SGM) that provides photons with energies in the range (30–1000) eV. The experiments were performed with a resolution better than 0.1 eV for the oxygen K-edge and Ca L-edge and 0.15 eV for the Cu $L_{2,3}$ -edges and Ce $M_{4,5}$. Polycrystalline samples were *in situ* scraped to get clean fresh surfaces. The pressure in the XANES experimental chamber was about 1×10^{-10} Torr. The spectra were recorded by detecting the total electron yield (TEY) from the samples drain current. TEY is a surface-sensitive technique, unlike the x-ray fluorescence yield (XFY) which is a bulk-sensitive measurement. Therefore TEY data do not require self-absorption correction [33]. The I_0 signal from a gold grid upstream from the beamline was also recorded for normalization purposes and to monitor the energy calibration from the Cr $L_{2,3}$ -edges' absorption signal in I_0 which originates from the Cr on the beamline gratings. The samples were mounted to a molybdenum holder with UHV-compatible double-sided conductive tape. Background subtraction was performed using a linear background fit for the energy region prior to each absorption edge. 600 l mm^{-1} spherical gratings were used for the measurements of the O K- and Ca $L_{2,3}$ -edges while a 1200 l mm^{-1} grating was used to measure both Ce $M_{4,5}$ and Cu $L_{2,3}$ -edges. The monochromator was calibrated by running x-ray photoemission spectra (XPS) for Au samples at different photon energies.

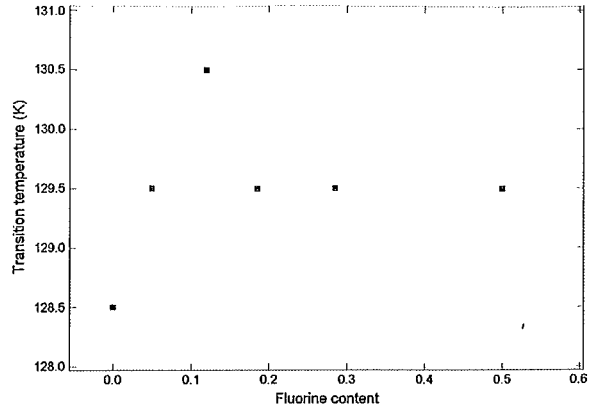


Figure 1. Variation of the transition temperature T_c of Hg-1223/ F_x with nominal fluorine content x .

3. Results and discussions

3.1. Anion substitution (fluorine for oxygen) in Hg-Pb-12223 system

3.1.1. Oxygen K-edge. Effect of fluorine substitution on the superconducting properties of $\text{Hg}_{0.8}\text{Pb}_{0.2}\text{Ba}_2\text{Ca}_2\text{Cu}_3\text{O}_y/\text{F}_x$ (HgPb-1223/ F_x) with $x = 0.00, 0.05, 0.120, 0.185, 0.285$ and 0.500 was investigated. We have found an increase in T_c as F was introduced into the structure of the Pb-substituted Hg-1223 [26]. Furthermore, the critical current density and both its magnetic field and temperature dependence were found to be greatly enhanced for both the Pb- and Re-doped Hg-1223 as fluorine was introduced [26, 27]. These improvements in the superconducting properties are believed to be due to changes in the charge carrier concentration in the CuO_2 planes and improvement of the inter- and intra-grain pinning mechanism. These conclusions were made based on the variation of the superconducting, electrical, magnetic and structural properties of the system as fluorine was introduced [26, 27]. In this study, we have directly probed the density of holes in various planes of this system by measuring the O K-edge and Cu $L_{2,3}$ -edges as a function of fluorine. Figure 1 shows the variation of T_c of Hg-1223/ F_x samples with fluorine content x . T_c increases for low fluorine content and then slightly drops, then saturates. T_c values were obtained from magnetic measurements using a SQUID magnetometer. Details of characterizations are published elsewhere [26, 27]. The samples were single phase with a superconducting volume fraction of more than 95%.

Figure 2 shows the O K-edge XANES spectra for HgPb-1223/ F_x with different F content x . The pre-edge peak A at about 528.3 eV is attributed to the transition of O 1s electrons to O 2p holes in the CuO_2 planes from $3d^9L \rightarrow O 1s3d^9$ (L denotes a hole on the O $2p_{x,y}$ orbital) states corresponding to the creation of a core hole on the O 1s level and filling of O $2p_{x,y}$ states located in the CuO_2 planes near the Fermi level. The assignment of this peak to the O $2p_{x,y}$ symmetry rather than the out-of-plane O $2p_z$ symmetry is confirmed by several polarization studies [14, 34–37]. Chen *et al.*, for example found that the intensity of this pre-edge peak in Tl-2223 decreases with increasing the polarized light's incident

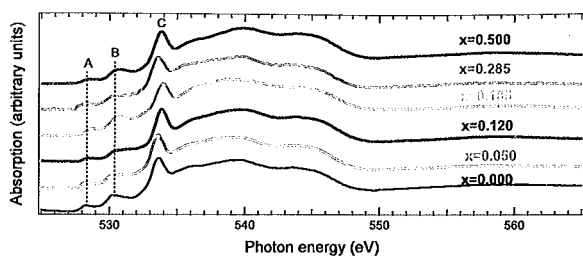


Figure 2. O K-edge of HgPb-1223/F_x as a function of fluorine content *x*.

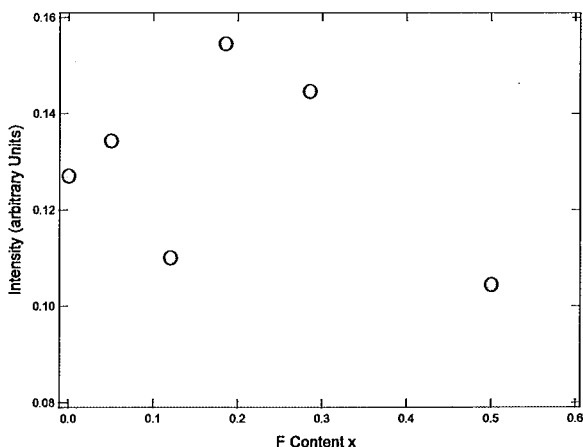


Figure 3. Variation of the intensity of the pre-edge peak in the O K-edge (feature A in figure 2) with F content *x*.

angle with the *c* axis [31]. The intensity of this peak in figure 2, slightly increases with increasing fluorine content up to an optimum value of *x*, as shown in figure 3. The behavior of this peak for the sample with *x* = 0.120 is inconsistent with other samples. This behavior could be attributed to the lack of homogeneity of this particular small piece of the sample that had been used for XANES measurement. The changes

in the intensity of this peak are responsible for fine-tuning the hole content in the CuO₂ planes, mostly by filling the vacant oxygen site in the Hg–O planes with fluorine [25]. The pre-edge peak B, at about 530 eV, is ascribed to the transition of O 1s to O 2p holes in the Ba–O planes. This peak could also be associated with the transition of the Cu 3d states hybridized with the O 2p states to the upper Hubbard band [38, 39]. Peak C is ascribed to O 2p holes in the Hg–O planes [17]. The spectral features above 535 eV reveal information about the local density of unoccupied states corresponding to O 2p states hybridized with Cu 4sp and Ba/Ca intermixing [34–39], HgPb-1223 has four nonequivalent oxygen sites: O(1) and O(1) within the CuO₂ layers of the square planar and pyramidal arrangements, respectively, O(2) in the Ba–O and O(3) in the Hg–O planes [26, 31, 32, 36].

3.1.2. Cu L_{2,3} edges. The Cu L_{2,3} absorption spectra of HgPb-1223/F_x as a function of fluorine content *x* are shown in figure 4(a) in the energy range (920–960) eV. The spectra consist of two main white lines at 931.3 eV and a wider peak at about 952 eV. A high energy shoulder of the main two peaks and a wide structure at about 943 eV are present. This wide feature is only clear in the fluorine-free sample and samples with low fluorine content and is absent in the spectrum of samples with higher fluorine content. The main white lines are ascribed to the transition from Cu(2P_{3/2,1/2})3d⁹–O 2p⁶ ground state into the Cu(2P_{3/2,1/2})⁻¹3d¹⁰–O 2p⁶ excited state, where (2P_{3/2,1/2})⁻¹ denotes a 2P_{3/2}, or 2P_{1/2} hole. These transitions are due to divalent copper, i.e. Cu^{+II} state. The high energy shoulder of both the L₂ and L₃ edges are due to copper in the trivalent state and attributed to the transition of Cu(2p_{3/2,1/2})3d⁹L ground state into the Cu(2p_{3/2,1/2})⁻¹3d¹⁰L excited state, where L denotes a ligand hole in the O 2p orbital [37–40].

The variation of the intensity of the Cu^{+III}/Cu^{+II} is shown in figure 4(b). The figure shows that the intensity of the Cu^{+III} peak increases as fluorine content was increased beyond *x* = 0.2 as a result of F incorporation into the structure. This means that there will be more O 2p holes in the Cu–O planes.

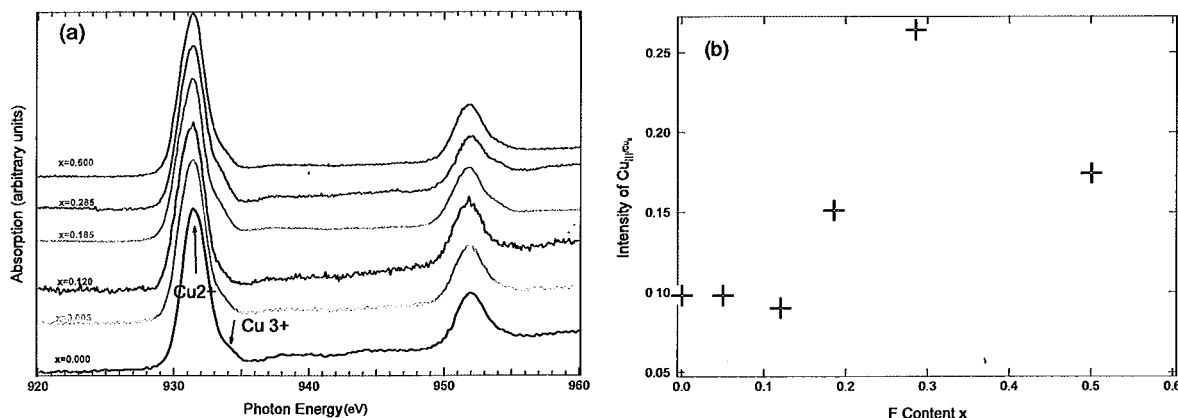


Figure 4. (a) Cu L_{2,3}-edge of HgPb-1223/F_x as a function of fluorine content *x*. (b) Intensity of the high energy shoulder (Cu³⁺) relative to the main peak (Cu²⁺).

In other words, the hole concentration in the CuO_2 planes of the under-doped HgPb-1223 has been increased through fluorine addition. The behavior of this high energy shoulder resembles and confirms the behavior of the pre-edge peak in the O K-edge spectra that occurs at about 528.3 eV and therefore supports the above assignment of the high energy shoulder in the Cu L_3 -edge spectra to be coming from the O 2p hole states. It is known that the interstitial oxygen site O(3) in the Hg-O plane of Hg-1223 is almost vacant [25–27]; therefore addition of fluorine will fill this empty oxygen vacancy and hence increases the number of holes in the CuO_2 planes in the originally under-doped compound. Due to the high ionic and electronegative nature of F^- , it will show less hybridization with mercury and thus each fluorine ion will donate nearly one hole to the CuO_2 planes [21, 22, 25, 26]. This is unlike what happens in the case of fluorine addition to Tl-1223 with similar structure [1]. In Tl-1223 the corresponding oxygen site in the Tl-O plane is almost fully occupied but the site in the CuO_2 plane is partially filled. Therefore in the case of Tl-1223, fluorine will first fill these partially filled states in the CuO_2 planes, and therefore reduces the hole concentration in the CuO_2 planes of the originally over-doped Tl-1223 compound [1, 21–24]. Further addition of fluorine beyond the optimum value will push the hole concentration in Hgpb-1223 towards the over-doped side, and in the Tl-1223 towards the under-doped side of the bell-shaped phase diagram that is well established between the number of holes in the CuO_2 planes and the superconducting properties (T_c) [3]. This is also in agreement with the behavior of the Cu L_3 -edge and O K-edge pre-edge structure in figures 2 and 4. These observations of the increase of the number of holes in CuO_2 planes are consistent with our earlier observations of the improvements of the superconducting properties of the samples through fluorine addition [26, 27]. Furthermore, the improvements of the critical current density are also related to the number of holes in the CuO_2 planes. It is also useful to mention at this point that the mechanism of hole doping through fluorine inclusion has also been affected as is clear from the improvements in both the field and temperature dependence of the magnetic hysteresis width published earlier at both low (intra-grain pinning) and high (inter-grain pinning) magnetic fields [26].

3.1.3. Ca $L_{2,3}$ -edge. Figure 5 shows the x-ray absorption spectra for the Ca $L_{2,3}$ -edge of Hg-Pb-1223/ F_x for samples with different fluorine content x . The figure is plotted in order of increasing fluorine in the upwards direction, starting with $x = 0$ for the lower curve. The structures in the spectra are mainly attributed to the $2p^63d^0$ to $2p^53d^1$ transition and did not show sensitivity to fluorine substitution, because there is no Ca-O plane in the structure of the Hg-1223 system. There are four clearly resolved features in the spectra at about peak A at 345 eV, peak B at 347.2 eV, peak C at 348.7 eV and peak D at 350.5 eV, plus two shoulders at the low energy side of the main peaks (B and D), at 346.1 and 349.3 eV. The splitting between the two main peaks B and D is 3.3 eV, corresponding roughly to the spin-orbit splitting of Ca 2p cores. The splitting of each edge into two peaks A and B for L_3 and C and D for L_2 is evidence of the presence of a crystal field at Ca sites, and

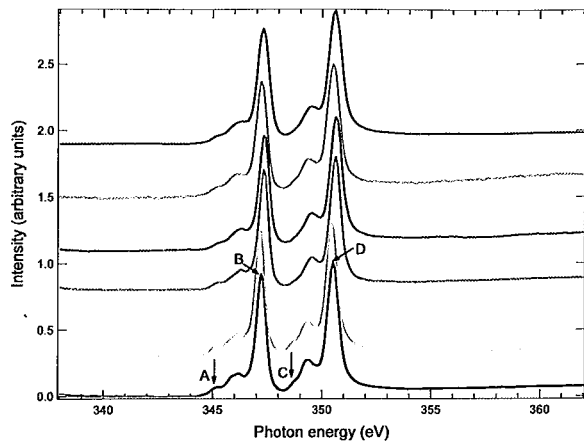


Figure 5. Ca $L_{2,3}$ -edge for Hg-Pb-1223/ F_x .

shows that Ca in HgPb-1223, as in Bi-2223 and in Bi-2212, behaves in a nonmetallic manner, although the crystal field is more clear in the case of Bi-2212 [41, 42].

The existence of crystal field splitting of Ca 3d levels had been shown for various Ca compounds [42]. They have found a clear crystal field splitting for ionic compounds such as CaO and CaF_2 . They have also found that there is no crystal field splitting in the Ca $L_{2,3}$ spectra of Ca in a metallic environment such as CaSi_2 [42]. The Ca $L_{2,3}$ -edge structure and crystal field splitting in HgPb1223/ F_x is more similar to CaF_2 and CaO. Ca in CaO has a sixfold coordination, while Ca in CaF_2 resides in a nearly cubic eightfold coordination as in the case in Bi-2212 [41]. The same argument is also true for Hg-Pb-1223/ F_x . In both compounds Ca is located between two CuO_2 planes. Therefore the peak splits off towards lower energy, i.e. peaks A and C can be assigned to the e_g orbital while peaks B and D are assigned to the t_{2g} orbital [41].

Figure 5 also shows two shoulders in the XANES Ca L -edge spectra of HgPb-1223/ F_x samples at the lower energy side of the main peaks B and D. These features have also been observed in CaF_2 , Bi-2212 and Bi-2223. Various authors attributed these features to Sr/Ca mixing at the Ca site with the transition from a $2p^63d^04s^1$ to $2p^53d^14s^1$ states that corresponds to Ca^+ instead of Ca^{2+} ions. We also attribute these features for HgPb-1223/ F_x to the same transition, as the structure of the Ca-O sub-lattice is similar in each of HgPb-1223/ F_x and Bi-2212 [41, 42]. The crystal field splitting observed for HgPb-1223/ F_x compounds in other systems was not observed in Y-doped Tl-Pb-1212 compound [43].

3.2. Cation substitution, $(\text{Tl}_{0.5}\text{Pb}_{0.5})\text{Sr}_{2-x}\text{Ce}_x\text{Ca}_2\text{Cu}_3\text{O}_{10}$ system

3.2.1. Oxygen K-edge. The resistivity measurement [8, 9] showed that there was an initial increase of the transition temperature T_c for the sample with $x = 0.1$ followed by a decrease in the transition temperature. Superconductivity vanished for the sample with $x > 0.3$, indicating a severe change in the hole concentration in the CuO_2 planes as Ce

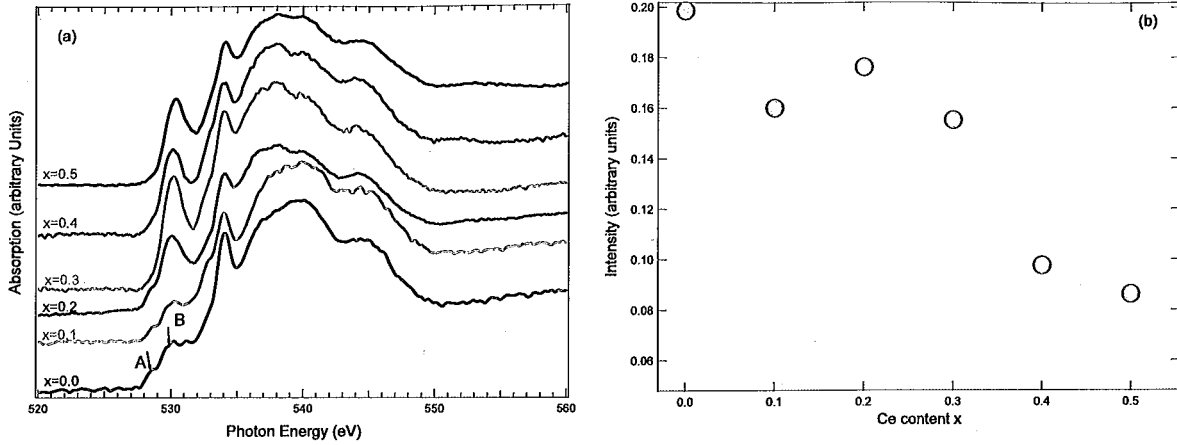


Figure 6. (a) O K-edge XANES spectra for $(\text{Tl}_{0.5}, \text{Pb}_{0.5}) \text{Sr}_{2-x}\text{Ce}_x\text{Ca}_2\text{Cu}_3\text{O}_y$ system for different values of x . (b) Intensity of the pre-edge feature (A) with Ce content x .

with a valence state higher than $2+$ replaces Sr^{2+} in the SrO planes [9]. Magnetic measurements showed a decrease in the magnetic hysteresis width as Ce content was increased, indicating that Ce incorporation at the Sr site does not enhance the phase formation of the superconducting phases [8, 9]. The superconducting fraction of the samples was decreased drastically for Ce content $x > 0.1$.

Figure 6(a) shows the normalized O K-edge x-ray absorption spectra for $(\text{Tl}_{0.5}\text{Pb}_{0.5}) \text{Sr}_{2-x}\text{Ce}_x\text{Ca}_2\text{Cu}_3\text{O}_{10}$ of different Ce content x . The spectra shown in this work were collected using the drain current mode.

The spectra had been normalized to the incident photon intensity (J_0) measured simultaneously by an Au mesh located upstream after the exit slit and the refocusing mirror. All spectra were then normalized so that they have the same absorption at the energy 560 eV, where there is no feature associated with the oxygen K-edge of these compounds.

These spectra are indications of the projected local density of unoccupied states on the O sites. Therefore, the region very close to the absorption edge is a measure of O 2p hole concentration in the valence band. The spectra are the superposition of unoccupied states that arise from Cu–O, Ca, Sr(Ce)–O and Tl(Pb)–O layers. The pre-edge structure is attributed to transitions from O 1s core states to holes with 2p symmetry on the oxygen sites. The first pre-edge starts at about 527.4 eV, which corresponds to the Fermi level.

The first feature in the pre-edge structure is a peak at about 528.6 eV and could be assigned to arise from Cu–O layers. It can be ascribed to the transition from $3d^9L \rightarrow \text{O } 1s3d^9$ (L denotes a hole on the O $2p_{x,y}$ orbital) states corresponding to creation of a core hole on the O 1s level and filling of O $2p_{x,y}$ states admixed to the upper Hubbard band. This transition is strongly related to the hole concentration in CuO_2 and is identical to the corresponding peak discussed above for $\text{HgPb-1223}/F_x$ [34–40].

Our samples consist of a mixture of Tl-1223 and Tl-1212 phases. It is well established that as-prepared Tl-1223 samples are always mixed with the Tl-1212 phase. In particular, it

was found to be impossible to obtain a Ce-doped Tl-1212 or Tl-1223 phase [1, 8, 9, 44, 45]. At the same time, both Tl-1223 and Tl-1212 superconducting phases are over-doped and have similar layered structures, especially from the hole concentration and Cu valence point of view. Therefore, our x-ray absorption results will not distinguish the O K-edge, Cu L-edge and Ce M-edge XANES spectra for the two phases. The valence state of Cu for both phases is the same ($2.2+$) [1, 5, 45].

In figure 6(b), we present the variation of the intensity of the pre-edge peak at about 528.6 eV with Ce content x . The figure shows a decrease of the peak's intensity as the Ce content x is increased which is a direct measure of hole concentration in CuO_2 planes and a confirmation of our earlier expectations that the hole concentration in CuO_2 planes decreases as Ce (in the valence state Ce^{3+} and Ce^{4+}) replaces Sr^{2+} in the metallic layer Sr–O. As Ce exists in a mixed valence state of $+3$ and $+4$, as we will see later in this paper, and because the unsubstituted sample is in the over-doped (over-oxidized) state, the valence state of Cu will be reduced, and therefore T_c will initially increase to a maximum value as the density of holes goes through its maximum and then decrease as we cross to the under-doped state. This result is in agreement with our measurement of the variation of the transition temperature of these samples with Ce content x [8, 9]. The increment of the Ce content x in this study seems to be very large. To scan the variation of the hole concentration with the T_c , we are working on substituting La in much smaller increments in the Sr site, rather than Ce. Initial measurements indicate that T_c gradually increases to reach a maximum value as the La content was increased. XANES measurements for the La-substituted Tl-1223 are being planned.

The assignment of the first pre-edge peak at 528.6 eV for the O(1) and O(1') agrees with local density-of-states calculations (LDA) of Tl-2223 by Marksteiner *et al* and also agrees with several authors for various Tl-based, Hg-based and Bi-based superconductors as these systems have similar structures [31, 32, 36]. Following the same reasoning

and utilizing the results of the LAD calculations [36], we can ascribe the second pre-edge feature at 529.4 eV with the O 2p holes in O(2) site of the Sr-O planes. These holes are with predominantly O 2p_z symmetry, as proven by polarization effects. The intensity of this peak increased on going from E1|*ab* to E1|*c* polarization, i.e. this peak has O 2P_z symmetry [31, 34].

The third pre-edge peak at about 530 eV is ascribed to the O 2p holes in the O(3) atoms within the Tl-O plane. This is consistent with the above discussions and results obtained for various Tl-based and Hg-based phases in both single crystals and polycrystalline samples [31, 46].

3.2.2. Ce M_{4,5}-edge. X-ray absorption spectra (XAS) spectra at the Ce M_{4,5}-edge is shown in figure 7. The spectra exhibit two main peaks known to be due to 3d_{3/2} (M₄) and 3d_{5/2} (M₅) multiplet structures of the 3d⁹4f² final state (M₅ main peak at 883.1 eV and M₄ main peak at 901.1 eV). The Ce M-edge spectra are well separated (~18 eV) due to large spin-orbit splitting between M₄ and M₅. Features at the higher energy side of the main peaks separated by (~5 eV) from the main peaks are driven by Coulomb interactions between the 3d core hole and the 4f sub shell, and by the Coulomb repulsion between 4f electrons. These two features are believed to arise from the transition from the initial ground state to the 3d⁹4f¹ final state [47]. These secondary peaks in (Tl_{0.5}, Pb_{0.5}) Sr_{2-x}Ce_xCa₂Cu₃O_y are very similar to those observed in CeCo₂, CeRh₂ and CeRh₃ and are indicative of a mixed valence state of Ce in these solid solutions. Therefore, we believe that the Ce state is a mixture of Ce⁴⁺ and Ce³⁺ in these samples. This result was also observed in Ce-doped-Bi-1223.223 [48]. The ground state of Ce in the Tl-1223-Ce compound can be described as a mixture of the 4f⁰ and 4f¹ states, such that the Ce M_{4,5}-edge in the XANES spectra exhibits a peak corresponding to the transition $i \rightarrow 3d^9 4f^1$ at 888 eV and 906.1 eV, respectively, and $i \rightarrow 3d^9 4f^2$ at about 883 and 906.1 eV, where i is the initial ground state. The intensity ratio of the high energy shoulder ($i \rightarrow 3d^9 4f^1$) transition to that of the main peak ($i \rightarrow 3d^9 4f^2$) does not change as the Ce content x was increased in the samples (about 0.6), indicating that the average Ce valence does not change, from sample to sample.

In summary, the Ce M_{4,5} XAS spectra show that Ce exists in a mixed valence state of 3+ and 4+. This result is a confirmation of previous expectations for the valence state of Ce in Tl-1212 [49, 50]. As this state is larger than that of Sr (2+), this will lead to hole filling, and hence a decrease in the valence state of Cu in the Cu-O₂ planes.

4. Conclusions

In this study, we have found that the hole concentration in the Cu-O₂ planes of Pb-doped Hg-1223 (HgPb-1223/F_x) increases with fluorine addition. As we have indicated in earlier studies fluorine should be replacing the interstitial oxygen site in the Hg-O plane, which has low occupancy in order to contribute to the increase of the hole concentration in the CuO₂ planes. The variation of the peak intensity of the pre-edge feature of

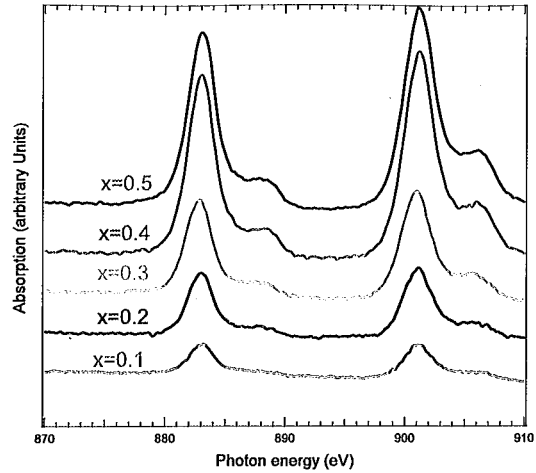


Figure 7. Ce M_{4,5}-edge for (Tl_{0.5}, Pb_{0.5}) Sr_{2-x}Ce_xCa₂Cu₃O_y system for different values of x .

the O K-edge associated with the number of O 2p holes in the CuO₂ layers and the intensity of the high energy shoulder in the Cu L₃ absorption edge increase gradually before they start decreasing for higher fluorine content. The presence of a crystal field as evident from the multiple structures of the Ca L₂ and L₃ edges shows that Ca behaves as nonmetallic in this system. The above results are in agreement with our observed improvements in the superconducting properties of these systems [1, 26, 27].

Furthermore, we have found that Ce substitution in the over-doped Tl-1223 system ((Tl_{0.5}, Pb_{0.5}) Sr_{2-x}Ce_xCa₂Cu₃O_y) decreases the number of holes in the Cu-O₂ planes gradually to the under-doped regime. This was clear from the behavior of the intensity of the pre-edge peak in the O K-edge structure for samples with different Ce contents. The Ce M_{4,5} XAS structure showed that Ce exists in a higher valence state (3+ and 4+) compared to Sr (2+), leading to the observed reduction in the number of holes in the Cu-O₂ planes and hence affecting the superconducting properties such as the transition temperature.

Acknowledgments

The Hg-based samples used in this work were prepared during the sabbatical leave of NMH at the National High Magnetic Field Laboratory in collaboration with Professor Justin Schwartz and Dr Sastry Pamidi. This work was partially funded from the DOE-BES. NMH would like to acknowledge the support of the Abdus Salam ICTP in Trieste, Italy. Special thanks are due to Dr M Faiz, and Dr S B Mun for their help in the data collection and discussions.

References

- [1] Hamdan N M, Ziq Kh A and Al-Harathi A S 1999 *Physica C* 314 125
- [2] Karppinen M, Kotiranta M, Yamauchi H, Nachimuthu P, Liu R S and Chen J M 2001 *Phys. Rev. B* 63 184507

- [3] Paranthaman M P, Manthiram A and Goodenough J B 1994 *Thallium-Based High Temperature Superconductors* ed A M Herman and Y J Yakhmi (New York: Dekker) p 171
- [4] Pan M H and Greenblatt M 1991 *Physica C* **176** 80
- [5] Liu R S and Edwards P P 1994 *Thallium-Based High Temperature Superconductors* ed A M Herman and J Y Yakhmi (New York: Dekker) pp 325–46
- [6] Hamdan N M, El-Ghanem H and Schwartz J 2000 *IEEE Trans. Appl. Supercond.* **10** 1174
- [7] Hamdan N M, Ziq Kh A, Al-Harathi A S and Shirokoff J 1998 *J. Supercond.* **11** 95
- [8] Hamdan N M 1999 *J. Low Temp. Phys.* **117** 1187
- [9] Hamdan N M 2000 *IEEE Trans. Appl. Supercond.* **10** 1170
- [10] Hamdan N 2000 *Physica B* **284–288** 1093–4
- [11] Putlin S N, Antipov E V, Chmaissem O and Marezio M 1993 *Nature* **362** 226
- [12] Sekhar B R, Studer F, Garg K B, Moriwaki Y, Gasser C and Tanabe K 2001 *Phys. Rev. B* **56** 134506
- [13] Marezio M, Capponi J J, Radaelli P G, Edwards P P, Armstrong A R and David W I F 1994 *Eur. J. Solid State Inorg. Chem.* **31** 843–54
- [14] Alonso R E, Rodrigues C O and Christensen N E 2001 *Phys. Rev. B* **63** 134506
- [15] Singh D J and Pikett W E 1994 *Phys. Rev. Lett.* **73** 476
- [16] Novokov D L and Freeman A J 1993 *Physica C* **216** 273
- [17] Serquis A, Caneiro A, Basset A, Short S, Hodges L P and Jorgensen J 2001 *Phys. Rev. B* **63** 14508
- [18] Sastry P V P S S, Amm K M, Knoll D C, Peterson S C and Schwartz J 1998 *Physica C* **297** 223
- [19] Sastry P V P S S and Schwartz J 1998 *J. Supercond.* **11** 592
- [20] Fabrega L, Fontcuberta J, Serquis A and Caneiro A 2001 *Physica C* **356** 254–60
- [21] Hamdan N M, Ziq Kh A and Al-Harathi A S 1996 *J. Low Temp. Phys.* **105** 1493
- [22] Faiz M and Hamdan N M 2000 *J. Electron Spectrosc. Relat. Phenom.* **107** 283
- [23] Hamdan N M and Faiz M 2001 *J. Electron Spectrosc. Relat. Phenom.* **114–116** 291–4
- [24] Hamdan N M, Al-Harathi A S and Choudhary M F 1997 *Physica C* **282–287** 2273–4
- [25] Peacock G B, Gameson I, Slaski M, Capponi J J and Edwards P P 1997 *Physica C* **289** 153
- [26] Hamdan N M, Sastry P V P S S and Schwartz J 2002 *IEEE Trans. Appl. Supercond.* **12** 1132–5
- [27] Hamdan M, Sastry P V P S S and Schwartz J 2000 *Physica C* **341–348** 513
- [28] Putlin S N, Antipov E V, Abakumov A M, Rozova M G, Lokshin K A, Pavlov D A, Balagurov A M, Sheptyakov D V and Marezio M 2000 *Physica C* **338** 52
- [29] Lockshin K A, Pavlov D A, Putlin S N, Antipov E V, Sheptyakov D V and Balagurov A M 2001 *Phys. Rev. B* **63** 64511
- [30] Wang Y T and Hermann A M 1995 *Physica C* **254** 1
- [31] Chen J M, Liu R G, Liu R S, Lin H C, Uen T M, Juang J Y and Gou Y S 1997 *Chem. Phys. Lett.* **276** 303
- [32] Pellegrin E, Fink J, Chen C T, Xiong Q, Lin Q M and Chu C W 1996 *Phys. Rev. B* **53** 2767
- [33] Kawa J *et al* 2000 *Spectrochim. Acta B* **55** 1385–95
- [34] Liu R S, Chen J M and Shy D S 1997 *Inorg. Chem.* **36** 1378
- [35] Saini N L, Law D S-L, Pudney P, Srivastava P, Menovsky A, Franse J J M, Ohkubo H, Akinaga H, Studer F and Garg K B 1995 *Physica C* **251** 7
- [36] Marksteiner P, Yu J, Massidda S and Freeman A J 1998 *Phys. Rev. B* **39** 2894
- [37] Chen J M, Liu R S and Hu S F 1996 *Physica C* **272** 180
Chen J M, Chung S C and Liu R S 1996 *Solid State Commun.* **99** 493
- [38] Chen J M, Liu R S and Linag W Y 1996 *Phys. Rev. B* **54** 12587
- [39] Karppinen M, Kotiranta M, Nakane T, Yamauchi H, Chang S C, Liu R S and Chen J M 2003 *Phys. Rev. B* **67** 134522
- [40] Karppinen M, Yamauchi H, Nakane T, Fujinami K, Lehmus K, Nachimuthu P, Liu R S and Chen J M 2002 *J. Solid State Chem.* **166** 229
- [41] Qvarford M, Andersen J N, Nyholm R, van Acker J F, Lundgren E and Lindan I 1992 *Phys. Rev. B* **46** 14126
- [42] Himpfel F J, Karlsson U O, McLean A B, Terminello L J, de Groot F M F, Abbate M, Fuggle J C, Yarmoff J A, Thole B T and Sawatzky G A 1991 *Phys. Rev. B* **43** 6899
- [43] Liu R S and Chen J M 1998 *Supercond. Sci. Technol.* **11** 1028–31
- [44] Hong Q and Wang J H 1993 *Physica C* **217** 439–43
- [45] Nakajima S, Kikuchi M, Syono Y, Oku T, Nagase K, Kobayashi N, Shindo D and Hiraga K 1991 *Physica C* **182** 89–94
- [46] Krol A *et al* 1990 *Phys. Rev. B* **42** 2635–8
- [47] Vavassori P, Duo L, Chiaia G, Qvarford M and Lindau I 1995 *Phys. Rev. B* **43** 6899
- [48] Liang G, Yao Q, Zhou S and Katz D 2005 *Physica C* **424** 107–115
- [49] Hong Q and Wang J H 1993 *Physica C* **217** 439–43
- [50] Lee W H and Wang D C 1995 *Physica C* **253** 156–64

DISCLAIMER

This document was prepared as an account of work sponsored by the United States Government. While this document is believed to contain correct information, neither the United States Government nor any agency thereof, nor the Regents of the University of California, nor any of their employees, makes any warranty, express or implied, or assumes any legal responsibility for the accuracy, completeness, or usefulness of any information, apparatus, product, or process disclosed, or represents that its use would not infringe privately owned rights. Reference herein to any specific commercial product, process, or service by its trade name, trademark, manufacturer, or otherwise, does not necessarily constitute or imply its endorsement, recommendation, or favoring by the United States Government or any agency thereof, or the Regents of the University of California. The views and opinions of authors expressed herein do not necessarily state or reflect those of the United States Government or any agency thereof or the Regents of the University of California.

This work was supported by the U.S. Department of Energy under Contract No. DE-AC02-05CH11231